Comparison of charging control techniques for electrochemical energy storage systems

Alejandro Clemente
Institut de Robòtica i Informàtica Industrial
Universitat Politècnica de Catalunya
Barcelona, Spain
alejandro.clemente.leon@upc.edu

Ramon Costa-Castelló
Institut de Robòtica i Informàtica Industrial
Universitat Politècnica de Catalunya
Barcelona, Spain
ramon.costa@upc.edu

***Abstract*—This conference paper presents a comparison study between different charging techniques for energy storage systems. The work presents the application of charging methods in two different types of models, which are a dynamic nonlinear electrochemical and the well-known equivalent circuit model. For both cases, a controller is designed in order to analyze its performance, using the classical PID implemented in the vast majority of industry controllers. In order to validate its implementation, the case of an emerging technology in terms of energy storage has been considered, as is the vanadium redox flow battery. The models have been calibrated for later validation, using a particle swarm optimizer and a real dataset found in the literature. The controllers have been developed separately, considering the variables and characteristics of each model. Finally, a comparison of both controlled systems is presented.**

***Index Terms*—Charging techniques, Energy storage systems, Redox flow battery, Particle Swarm Optimization**

I. Introduction

Within the current energy situation, where the demand of large energy storage systems (ESSs) is growing exponentially, the use of electrochemical battery systems is one of the greatest solutions. The main benefit of this type of systems is that it can be implemented for energy storage in solar or wind plants with the necessary storage capacity, being used as secondary elements in these important renewable installations [1]. However, one of the main challenges in the study of electrochemical ESS is the determination of charging techniques.

The strategies used to determinate them are usually divided in two different types. On one hand, some strategies are focused on the search of fast and safe charging laws, which avoid the appearance of secondary reactions. For electrochemical typologies of ESSs such as lithium-ion batteries or redox flow batteries (RFBs), a simple charging technique consists on the use of a constant current-constant voltage (CC-CV) profile [2]. However, this strategy can lead to gassing side reactions or battery deterioration if these values are not regulated. For this reason, this strategy has been changed to one that consists on first introducing a constant current profile until the state of charge (SOC) reaches an upper bound, followed by a constant voltage profile until maximum SOC is reached [3].

On the other hand, there are strategies focused on the determination of charging methods that maximize the ESS efficiency, reducing the possible losses. Within this scenario, there are different studies that present optimal charging techniques, as for example the use of a negative pulse charging theory [4] or an optimal flow rate law that minimizes pump losses in RFBs [5].

Among all possible control strategies, the most typical ones are voltage and power tracking [6]. The main reason is that usually the energy demand of these variables depends on the systems or installations where they are connected. Thus, considering a microgrid where the RFB serves as a support element, the energy demand in terms of voltage and power is imposed by other devices such as the grid, solar panels or other ESSs.

Both strategies have been extensively analyzed for different types of ESS [7], seeking different goals but sharing the same starting point, which is the use of a mathematical model that can describe the real behaviour of the system and make it possible to analyze and formulate a control strategy.

Within electrochemical ESS modeling, the use of dynamic lumped parameter models (LPMs) stands out. The main reason for this is the simplification of the system analysis and formulation, unlike distributed models where the variables depend not only on the time but also on other spatial variables [8].

Within the scope of LPM, there exists another distinction, which is the use of physical or equivalent models [9]. On one side, a physical model is more realistic since, as its name suggests, its formulation is directly related with physical phenomena that can be computed by ordinary differential equations (ODEs). However, as many of these ODEs can hinder the theoretical analysis and could have a high computational cost, the use of equivalent models appears as a better option. The most common type of electrochemical systems is

This research was supported by the support from the CSIC program for the Spanish Recovery, Transformation and Resilience Plan funded by the Recovery and Resilience Facility of the European Union, established by the Regulation (EU) 2020/2094, CSIC Interdisciplinary Thematic Platform (PTI+) Transicion Energetica Sostenible+ (PTI-TRANSENER+ project TRE2103000), the Spanish Ministry of Science and Innovation under projects MAFALDA (PID2021-126001OB-C31 funded by MCIN/AEI/ 10.13039/501100011033 / ERDF,EU), and MASHED (TED2021-129927B-I00), and by the Spanish Ministry of Universities funded by the European Union - NextGenerationEU (2022UPC-MSC-93823).

the equivalent circuit model (ECM), which relies on the use of different electric components such as voltage/current sources, resistors and capacitors [10]. Considering their complexity, there are different typologies of ECMs, ranging from the simplest, which correspond to zero-order models composed by a resistor and a voltage source, to second or third-order models composed by different RC branches [11]. The main problem when dealing with ECMs is that their parameters are unknown and must be estimated in order to verify the reliability of the model. This parameter estimation is a challenge that has been analyzed by different studies as [12], where a particle swarm optimizer (PSO) is used to estimate the parameters of a lithium-ion battery ECM.

Based on these different models, the aim of this work is to propose and analyze, for each one of them, a charging technique that can solve typical challenges in electrochemical ESSs such as the voltage and power tracking or the minimization of side reactions. Thus, the goal is to propose different valid charging techniques that could be implemented in an electrochemical ESS, adapted to its corresponding model.

In order to properly analyze and validate the proposed controllers, a real electrochemical ESS consisting on a vanadium redox flow battery (VRFB) has been used as an example. This particular system has been chosen since it is being widely used in recent years. The main reason for this are its high efficiency (70-90%) [13], long life and the possibility of decoupling energy and power [14], when compared to other electrochemical ESSs.

The VRFB was designed by professor Skyllas-Kazacos [15], who pioneered the use of vanadium in RFBs and has actively participated in the analysis and study of this system. Most of her works are focused on the design and analysis of electrochemical and thermal models oriented to SOC estimation [16]. In terms of charging methods, the main advantage of VRFBs compared to other types of batteries such as lithium-ion batteries is that the control strategy can be defined considering a new variable besides from the current and voltage, which is the electrolyte flow rate. Taking this into account, a voltage control strategy for different currents is proposed in [17], consisting on a H_∞ flow rate controller.

This work allows to analyze two different studies. Firstly, it compares the ECM and the physical model, in terms of data fitting with the dataset used. Secondly, it makes it possible to develop a comparison of both models in terms of optimal charging techniques, being able to analyze under which conditions the use of an ECM or electrochemical model could be more appropriate. The development of optimal controllers has been analyzed in several works such as [18] that presents the use of multi-parametric quadratic programming in fuzzy control systems or [19] presenting the use of optimal controllers in nonlinear systems. However, in this work the purpose is to analyze the performance of classical PID controllers. In order to do that, there are works that present tuning rules for robust PID controllers [20]. However, in this work it is intended to use the particle swarm optimization (PSO) algorithm that makes possible to find solutions for non-convex problems as the one addressed, defining the measure of quality and possible constraints.

The work is organized as follows: Section II presents the formulation of the ECM and the physical electrochemical model for a VRFB. In Section III, both models are calibrated with real data found in the literature, solving the parameter estimation problem by means of a PSO. The design of optimal charging controllers is presented in Section IV, and Section V presents a comparative evaluation. Finally, the fruitful conclusions are summarized in Section VI.

II. Model formulation

A. Equivalent circuit model

Among the different typologies of ECMs that exist for the modeling of electrochemical systems such as batteries, the Thevenin first-order circuit is the most commonly used [21]. A scheme of this ECM is shown in Fig 1, where the different components can be appreciated. The voltage source represents the open circuit voltage (OCV), usually denoted as E^{OCV} in V units, the resistor R_0 allows to consider the ohmic losses, having units of Ω and the R_pC_p branch is used to model the polarization losses by means of a resistor R_p and a condensator C_P with units of Ω and F, respectively.

Thus, the computation of the battery terminal voltage E, can be formulated following the Kirchhoff's second law as:

$$E = E^{OCV} + R_0 \cdot I + E^p \ , \tag{1}$$

where I is the current in A units, being positive for a charging process and negative for a discharging one.

The term E^{OCV} is function of the SOC and can be computed by means of the Nernst equation as:

$$E^{OCV} = E^\theta + \frac{2RT}{zF} ln\left(\frac{SOC}{1-SOC}\right) \ , \tag{2}$$

being E^θ the standard electrode potential for a VRFB, which value is 1.4 V, R = 8.31 Jmol^{-1}K^{-1} the gas constant, F = 9.6485$\cdot$ 10^4 sA mol^{-1} the Faraday constant, T = 298 K the electrolyte temperature and z the number of electrons involved in the redox reaction which is 1 for a VRFB.

With respect to the term E^p of expression (1), it defines the polarization losses associated to the concentration and activation overpotentials. It can be computed by means of the following differential equation:

$$\dot{E^p} = \frac{I}{C_p} - \frac{E^p}{R_pC_p} \ . \tag{3}$$

Finally, the SOC can be computed as a function of the current and the battery capacity C_n as [22]:

$$\dot{SOC} = -\frac{I}{C_n} \ . \tag{4}$$

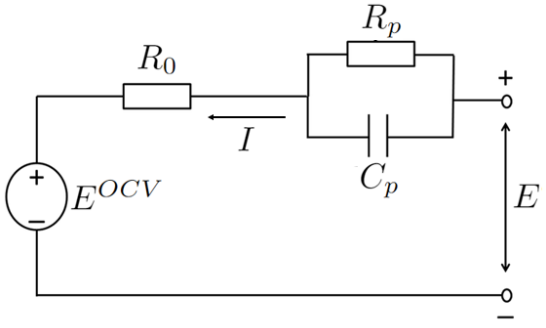

Fig. 1. Scheme of the first-order Thevenin ECM.

B. Dynamic electrochemical model

The electrochemical model presents the evolution of the vanadium species inside the cell and tanks. There are four species in a VRFB, which are V^{2+},V^{3+},VO^{2+} and VO_2^+. Their evolution along the time depends both on the charging/discharging current and on the electrolyte flow rates q with units of $m^3{\cdot}s^{-1}$. Therefore, based on the models proposed by Skyllas-Kazacos, the species evolution can be represented in the state-space notation as [23]:

$$\dot{\boldsymbol{x}} = \mathbf{A}\boldsymbol{x} \cdot q + \mathbf{b}I \ , \tag{5}$$

being $\boldsymbol{x} = [c_2^c, c_3^c, c_4^c, c_5^c, c_2^t, c_3^t, c_4^t, c_5^t]^\top$ the state vector where the sub-index indicates the species and the super-index is used to distinguish if the species concentration is inside the cell, denote with c, or inside the tank, denote with t. As can be noticed, matrix $\mathbf{A} \in \mathbb{R}^{8\times8}$ is related with the flow rate q while vector $\mathbf{b} \in \mathbb{R}^8$ is related with the current. Their expressions and details can be found in [23].

Based on the species concentration inside the cell, it is possible to compute the battery voltage E by means of the following expression:

$$E = N \cdot (E^{OCV} + R_0 \cdot I + \eta^{act} + \eta^{con}) \ , \tag{6}$$

which is similar to the ones of the ECM model (1) differing on the computation of the activation and concentration over-potentials, defined as $\eta^{act}$and η^{con}, respectively. Moreover, it is possible to compute the terminal voltage for a VRFB composed by different single cells N assembled in series.

For the particular case of a VRFB, the OCV depends on all vanadium species and can be computed as:

$$E^{OCV} = E^\theta + \frac{RT}{zF} ln\left(\frac{x_1 \cdot x_4}{x_2 \cdot x_3}\right) \ . \tag{7}$$

The activation over-potential η^{act} is formulated based on the Butler-Volmer equation [24]:

$$I = I_0 \left(e^{\frac{(1-\alpha)\cdot F}{RT}\eta^{act}} - e^{-\frac{\alpha \cdot F}{RT}\eta^{act}} \right) \tag{8}$$

being α the change transfer coefficient and I_0 the exchange current density that can be computed as follows:

$$I_0 = \frac{1}{s_e} \cdot \left(F \cdot k^\theta \cdot x_1^{1-\alpha} \cdot x_2^\alpha \cdot x_3^\alpha \cdot x_4^{1-\alpha}\right) \tag{9}$$

where s_e is the electrode surface in m^2 units and k^θ is the rate constant. Expression (8) defines a smooth implicit function $\eta^{act}(I, I_0, \alpha)$ that cannot be numerically isolated. For that reason, it has been approximated by means of a 2 piecewise function using the hyperbolic sine function [25]. The final expression is formulated as:

$$\eta^{act} = \begin{cases} \dfrac{RT}{(1-\alpha)F} hsin^{-1}\left(\dfrac{I}{I_0}\right) & \text{if } I/I_0 < 0 \\ \dfrac{RT}{\alpha \cdot F} hsin^{-1}\left(\dfrac{I}{I_0}\right) & \text{if } I/I_0 > 0 \end{cases} \tag{10}$$

For the case of the concentration over-potential η^{con}

$$\eta^{con} = \frac{RT}{zF} \begin{cases} ln\left(\dfrac{x_4 - |\Delta c|}{x_4}\right) - ln\left(\dfrac{x_1}{x_1 - |\Delta c|}\right) & I < 0 \\ ln\left(\dfrac{x_2 - |\Delta c|}{x_2}\right) - ln\left(\dfrac{x_3}{x_3 - |\Delta c|}\right) & I > 0 \end{cases}$$

where Δc is the concentration difference between the surface and bulk, which can be computed as:

$$\Delta c = \frac{I}{k_m F} \ , \tag{11}$$

being k_m the mass transfer coefficient.

With respect to the SOC, it is normally associated to the tanks species concentration. Thus, it can be computed for both sides of the system as:

$$SOC_- = \left(\frac{x_5}{x_5 + x_6}\right) \tag{12}$$

$$SOC_+ = \left(\frac{x_8}{x_7 + x_8}\right). \tag{13}$$

III. Model Calibration

Once the models have been formulated, it is important to determine the unknown parameters in order to be able to calibrate them. Thus, it is possible to analyze if these models resemble the real behavior of a VRFB. In order to develop this analysis, real data obtained from a charging and discharging experiment have been used.

The dataset in question is presented in [26], where different experiments are carried out with a VRFB composed by 10 single cells with an electrolyte composition of 1 M $VOSO_4$ in 4 M H_2SO_4. The volumes of the electrolyte tanks are 50 ml and the charging and discharging processes take place at a constant current of 0.3 A. Finally, the flow rate used in these experiments is 200 $ml{\cdot}min^{-1}$.

The data have been acquired every second and correspond to the current and voltage measurements. The experimental data selected consist on a discharging and charging profile at constant current as can be seen in Fig. 2.

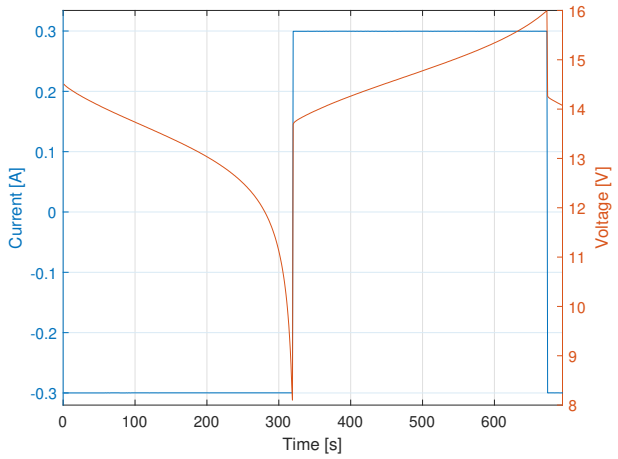

Fig. 2. Voltage and current measurements of the experimental data used.

With this experimental data it is possible to propose a PSO for each one of the models described. For both cases, the measure of quality is the absolute error between the real voltage and the estimated one.

A. ECM model calibration

According to the ECM presented, the parameters that must be estimated are the initial SOC and the resistors and capacitors R_0, R_p, C_p and C_n. Therefore, the set of parameters is defined as: $\mathbf{p} = [SOC(0), R_0, R_p, C_p, C_n]$.

Using this parameter vector, the optimization problem is formulated as follows:

$$\begin{aligned}
\min_{\mathbf{p}} \quad & \sum_{i=1}^{n_i} |E(i \cdot T_s) - \widehat{E}(i \cdot T_s)| \\
\text{subject to} \quad & \\
& \dot{\widehat{E^p}}(i \cdot T_s) = \frac{I(i \cdot T_s)}{C_p} - \frac{\widehat{E^p}(i \cdot T_s)}{R_p C_p} \\
& \dot{\widehat{SOC}}(i \cdot T_s) = -\frac{I(i \cdot T_s)}{C_n} \\
& \widehat{E}(i \cdot T_s) = \widehat{E^{OCV}}(i \cdot T_s) + R_0 \cdot I(i \cdot T_s) \\
& \qquad + \widehat{E^p}(i \cdot T_s) \\
& \mathbf{f}(\mathbf{p}) \leq \mathbf{0}.
\end{aligned}$$

being n_i the number of samples, T_s the sample period, E the measured voltage, $\widehat{E}$ the estimated one and $\mathbf{p}$ the set of the parameter constraints that is presented in TABLE I.

TABLE I
ECM PARAMETERS BOUNDS.

Parameter	LB	UB
$SOC(0)$	0	1
R_0	10^{-3}	10^2
R_p	10^{-3}	10^2
C_p	10^{-6}	10^{-2}
C_n	10^{-6}	10^{-2}

B. Dynamic electrochemical model calibration

Considering the electrochemical model, some assumptions can be made in order to relax the problem of estimating the 8 initial concentrations. Firstly, it is assumed that the electrolyte flow rate is high enough to not make a distinction between cell and tank dynamics. In fact, for the real VRFB presented, where the electrolytes volumes are 50 ml, a flow rate of 200 ml·min^{-1} is high enough to ensure this hypothesis. Thus, it is possible to remove four states from the original formulation.

Secondly, based on the matter and charge conservation principles, it is possible to eliminate two more states. Therefore, the simplified model corresponds to a second-order model with states x_1 and x_2.

Finally, the unknown parameter vector is composed by the initial states $x_1(0)$ and $x_2(0)$ and the unknown parameters R_0, α and k^θ. For this case the PSO problem is formulated as:

$$\begin{aligned}
\min_{\mathbf{p}} \quad & \sum_{i=1}^{n_i} |E(i \cdot T_s) - \widehat{E}(i \cdot T_s)| \\
\text{subject to} \quad & \dot{\widehat{\boldsymbol{x}}}(i \cdot T_s) = \mathbf{A}\widehat{\boldsymbol{x}}(i \cdot T_s) \cdot q + \mathbf{b} I(i \cdot T_s) \\
& \widehat{E}(i \cdot T_s) = h\left(\hat{\boldsymbol{x}}(i \cdot Ts), I(i \cdot Ts)\right) \\
& \mathbf{f}(\mathbf{p}) \leq \mathbf{0}.
\end{aligned}$$

where the vector parameter $\mathbf{p}$ is $[x_1(0), x_2(0), R_0, \alpha, k^\theta]$, and h is the battery voltage function in terms of the states and current I, which is expressed by means of (6).

For this second case, the parameter bounds appear summarized in TABLE II.

TABLE II
ELECTROCHEMICAL MODEL PARAMETERS BOUNDS.

Parameter	Lower bound	Upper bound
$x_1(0)$	0	10^3
$x_2(0)$	0	10^3
R_0	10^{-3}	10^2
α	0.4	0.6
k^θ	10^{-6}	10^{-2}

C. Calibration results

The optimization problems presented have been solved using Matlab with the PSO algorithm [25]. Thus, it is possible to solve the minimization problem considering the system constraints. For all problems it has been used a population of 100 particles and the $fmincon$ function.

The results are shown in Fig. 3, which displays the voltage profiles for both the ECM and electrochemical model, and the real voltage measurement E. As can be noticed, both profiles show good results in terms of fitting, specially in the intermediate charging area. However, when SOC is low, the ECM model presents a slight deviation with respect to the real profile, in contradistinction to the electrochemical model that presents a profile that is very similar even in this low SOC period.

The parameter vectors obtained can be compared in order to identify some relationships. On one hand, in the

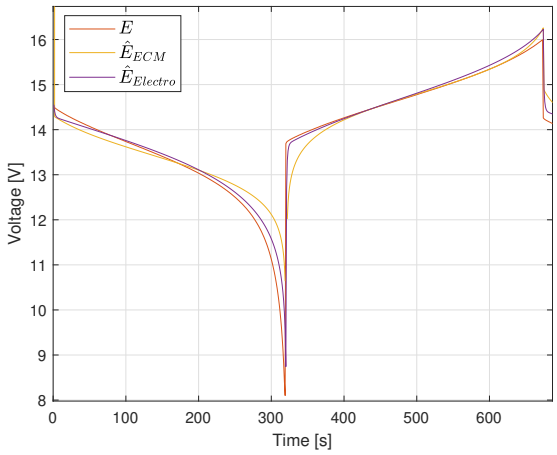

Fig. 3. Estimated voltages profiles for the ECM (yellow) and the electrochemical model (purple) compared to the real one (red).

case of the ECM model, the parameter vector estimated is $\mathbf{p} = [0.57, 0.027, 0.015, 0.00067, 0.67]$. On the other hand, considering the electrochemical model the parameter vector calibrated is $\mathbf{p} = [552, 448, 0.029, 0.52, 0.00045]$.

From these results, it is possible to see how the initial SOC of the ECM model has been estimated in 56%, while for the case of the electrochemical model, its value is 55.2% considering expression (12) for its computation. Another comparison that can be directly extrapolated is the ohmic resistance R_0, which has a value of 0.027 Ω and 0.029 Ω, respectively, for the ECM and the electrochemical models.

IV. Charging controller design

With the ECM and electrochemical models already calibrated, the next step consists on designing the optimal controller for each one of these models. At this point, it is important to remark that the ECM does not take into account the flow rate variable. Therefore, the controllers that can be designed using this model can only consider the current as the control action. On counterpart, considering the electrochemical model, it is possible to use both current and flow rate variables as control actions.

A. ECM charging controller

The first controller that can be easily implemented for the ECM consists on a tuned PID with the purpose of voltage tracking. Thus, it is possible to formulate an optimization problem that tries to obtain the optimal parameters of the well-known PID controller.

As the ECM is non-linear, common techniques such as the gradient descent methods are not viable as they are used to solve convex problems and the ones presented in this work are non-convex. For that reason, the PSO method is used in order to find a possible candidate that fits in the measure of quality defined.

As the purpose of this controller is to track a reference, the measure of quality used to design the optimization problem is the tracking error ε, which can be computed as:

$$\varepsilon = E_{ref} - E \,, \tag{14}$$

being E_{ref} the voltage reference profile.

Thus, the optimization problem can be described introducing a new parameter vector $\mathbf{p}$ that is related with the PID actions: $\mathbf{p} = [K_p, T_i, T_d]$ being K_p, T_i and T_d the proportional, integral and derivative actions.

$$\begin{aligned}
&\min_{\mathbf{p}} \quad \sum_{i=1}^{n_i} |\varepsilon(i \cdot T_s)| \\
&\text{subject to} \\
&\qquad \dot{\widehat{E^p}} = \frac{\varepsilon(i \cdot T_s) C(s)}{C_p} - \frac{\widehat{E^p}}{R_p C_p} \\
&\qquad \dot{\widehat{SOC}} = -\frac{\varepsilon(i \cdot T_s) C(s)}{C_n} \\
&\qquad \widehat{E} = \widehat{E^{OCV}} + R_0 \cdot \varepsilon(i \cdot T_s) C(s) + \widehat{E^p} \\
&\qquad \underline{I} \leq I \leq \overline{I} \\
&\qquad \mathbf{f}(\mathbf{p}) \leq \mathbf{0} \,.
\end{aligned}$$

where $C(s)$ is the PID controller introduced with a unit feedback in the system which is directly related with $\mathbf{p}$ by means of the following expression:

$$C(s) = K_p \left(\varepsilon + \frac{1}{T_i} \int \varepsilon(\tau) d\tau + T_d \frac{d\varepsilon}{dt} \right) \tag{15}$$

As has been done previously, it is necessary to define the constraint vector of parameters, which in this case is summarized in TABLE III.

TABLE III
PID bounds

Parameter	Lower bound	Upper bound
K_p	-10^{-4}	10^2
T_i	-10^{-6}	10^2
T_d	-10^{-6}	10^2

The tuned PID controller for the optimization problem formulated is the following one: $\mathbf{p} = [9.56, 0.0156, 0.0043]$. Applying this controller to the ECM model, considering as a reference voltage the experimental profile used to calibrate the system models, it is possible to analyze the system performance.

As can be noticed in Fig. 4, the output voltage tracks the desired reference. In the detail, it is possible to see how despite the sudden change of current from discharging to charging method, the voltage signal does not present any overshoot. In order to guarantee that the current control signal does not present values outside the permitted operating ranges, which could lead to an inappropriate charge, the PID controller has been designed considering a lower and upper bound for I, named $\underline{I}$ and $\overline{I}$, respectively. For the case presented, it has

been bounded between -2 and 2 A. Fig. 5 shows the control current profile, where it can be noticed how the current does not exceed these values, guaranteeing a safe charging.

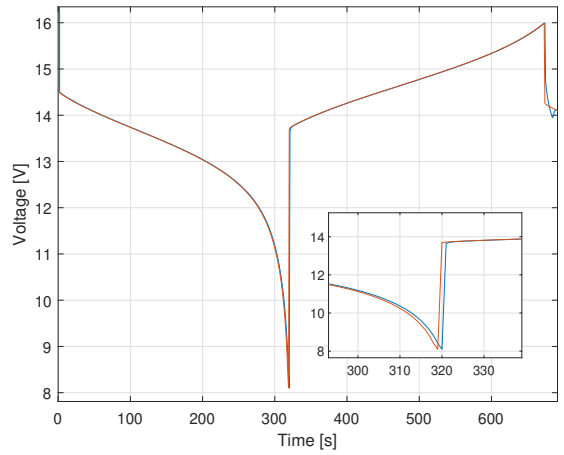

Fig. 4. Referenced (red) and controlled (blue) voltage profiles for the ECM.

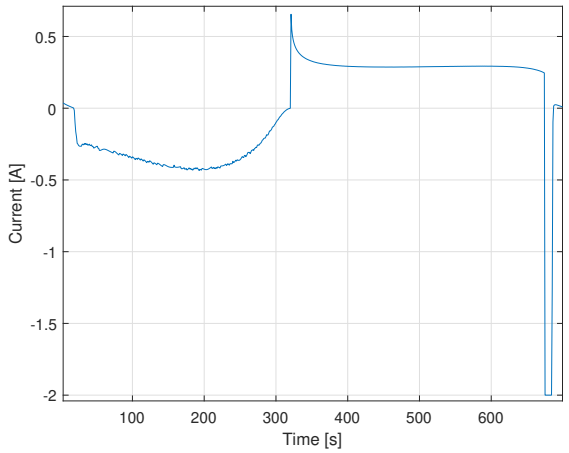

Fig. 5. Control current profile for voltage control for the ECM.

Another controller that can also be designed considering the ECM consists on the power control. In most cases, the purpose when using an ESS is ensure that can satisfy a power-energy demand. Thus, considering the power as a reference, the same optimization problem as the one presented previously has been used, substituting the voltage error ϵ for the power error defined as:

$$\varepsilon = P_{ref} - P, \tag{16}$$

being P the battery power computed as: $P = E{\cdot}I$. In that case, to ensure safety conditions, both current and voltage signals have been bounded.

For the case of the current the previous bound has been used, while for the voltage it has been used a bound between 8 and 18, corresponding to the values near the minimum and maximum SOC, respectively.

The power tracking problem has been analyzed applying a constant power profile that varies between -5 and 5 W. For this particular case, the PID controller obtained from PSO computation is $\mathbf{p} = [9.56, 0.0156, 0.0043]$. As can be noticed in Fig. 6, the required power is obtained using this controller, presenting only an initial fluctuation compared to the desired value when applied for first time and when the process changes from discharging to charging.

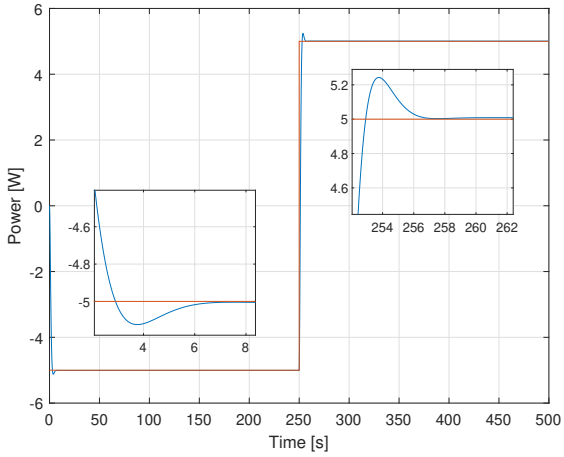

Fig. 6. Referenced (red) and controlled (blue) power profiles of the ECM controller.

To analyze the safe battery operation without overshoots in both current or voltage variables, their values have been also computed. Fig. 7 shows both profiles, where it can be noticed how the current does not overpass the 0.5 A, while the voltage is found between the 11 and 16 V, which are values that guarantees that none of the species concentrations are close to running out, which could be translated into the appearing of unwanted reactions.

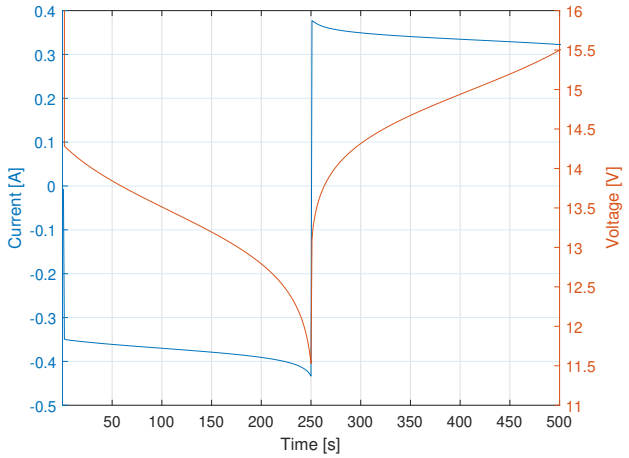

Fig. 7. Voltage and current profiles for power control using the ECM model.

B. Electrochemical model charging controller

Using the electrochemical model, it is also possible to develop a PID controller that is able to control previous battery variables such as the voltage o power.

If the aim is to control the battery power, the optimization problem that must be formulated is the following one:

$$\min_{\mathbf{p}} \quad \sum_{i=1}^{n_i} |\varepsilon(i \cdot T_s)|$$

$$\begin{aligned} \text{subject to} \quad & \dot{\hat{\boldsymbol{x}}}(i \cdot T_s) = \mathbf{A}\hat{\boldsymbol{x}}(i \cdot T_s) \cdot q + \mathbf{b}I(i \cdot T_s) \\ & \widehat{E}(i \cdot T_s) = h\left(\hat{\boldsymbol{x}}(i \cdot Ts), I(i \cdot Ts)\right) \\ & \underline{I} \leq I \leq \overline{I} \\ & \underline{E} \leq E \leq \overline{E} \\ & \mathbf{f}\left(\mathbf{p}\right) \leq \mathbf{0}\ , \end{aligned}$$

where ε is the power error that can be computed by means of (16). In that case, as can be noticed, both voltage and current variables have been bounded to avoid unwanted values, using the same bounds as the ones used for the ECM design. For this particular case, the tuned PID vector has been $\mathbf{p} = [12.34, 10.15, 0.012]$, obtaining the power profile obtained is presented in Fig. 8, where it can be seen that the results are quiet similar to the ones obtained using the ECM design.

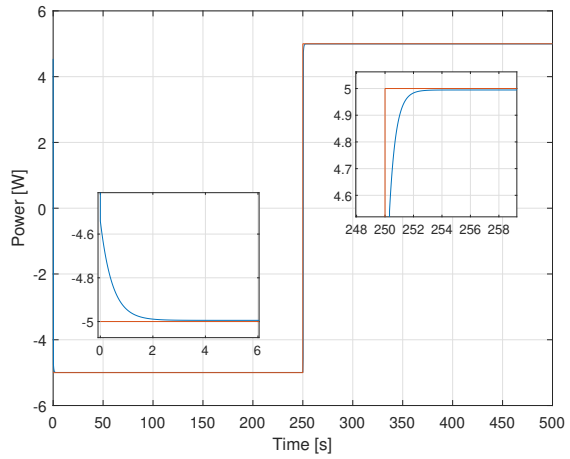

Fig. 8. Referenced (red) and controlled (blue) power profiles for the electrochemical model.

One of the strengths of using the electrochemical model is that the current and the eletrolyte flow rate can be used as control actions. Thus, it is possible to develop a new controller using this last variable. The same authors of this work have presented a voltage controller which is able to track a voltage profile, although the current presents abrupt changes, by means of controlling the electrolyte flow rates [27]. This controller was developed based on the H_∞ norm, but can also be computed using an industrial PID following the procedure done for previous controllers.

In order to validate this controller, a voltage profile has been used as reference, varying between 14 and 16 V, while a current profile with different changes have been also defined, which varies between 0.2 and 1 A. Fig 9 shows how the output voltage follows the reference with null steady-state error. It can be noticed how, in the presence of abrupt current changes, the controller works correctly regulating the flow rate. The current profile is shown in Fig. 10, jointly with the flow rate control signal.

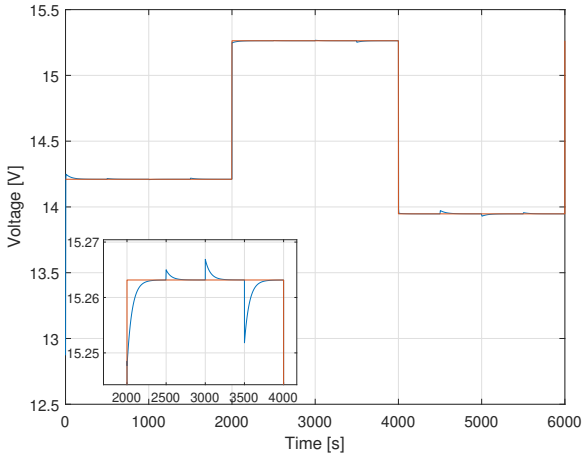

Fig. 9. Referenced (red) and controlled (blue) voltage profiles for the electrochemical model.

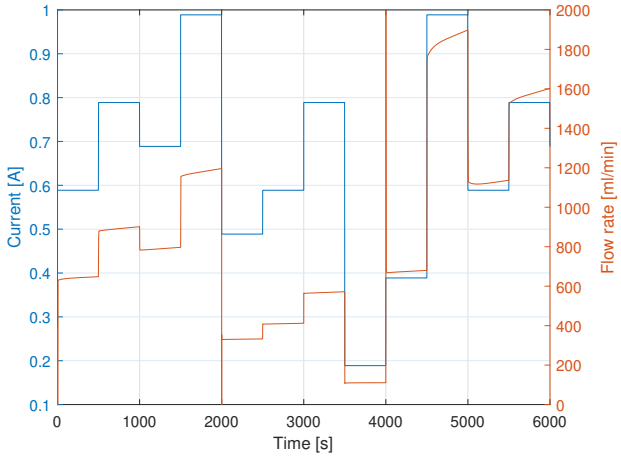

Fig. 10. Current and flow rates profiles for voltage control using the electrochemical model.

V. Comparative Evaluation

Considering the results obtained in the previous section, as well as the design procedure followed, some conclusions can be extrapolated. First of all, it is important to remark that the use of both ECM and electrochemical models for ESSs allows the implementation of traditional PID controllers for tracking problems such as voltage or power tracking. Moreover, the use of this types of models can be found in the literature for other purposes such as state and parameter estimation problems.

The design of the controllers by means of a optimization method as the PSO used in this work allows to implement and define a particular control problem for both models, facilitating the problem design. Nevertheless, the use of an electrochemical instead of an ECM allows to consider the flow rate as a control variable, giving more wealth in the control scope for other purposes such as the optimal control minimizing the mass imbalance or pump losses.

VI. Conclusions

This conference paper has presented a methodology to design traditional PID controllers that can be used in the control of electrochemical ESS. The control design has been carried out using two different types of models that are used in the field of battery modeling, obtaining positive results when both voltage and power control problems have been formulated. In order to solve these problems, the PSO algorithm has been used. One of the main advantages of this technique is the possibility to define the cost function and some constraints that are generally important in ESS problems such as the voltage or current limitation. However, it is important to remark that the performance of this technique depends on the operating conditions when the PID it is calibrated. Thus, the tuned controller is fragile when new experiments can be carried out with distant operational conditions or uncertainty. In order to analyze this problem, using the electrochemical model it has been possible to validate the tuned PID controller even in presence of sudden changes in the current variable that can be seen as system uncertainty. Moreover, it has been possible to analyze the benefits of using an electrochemical model instead of an ECM for voltage control with variable flow rates.

References

[1] L. Yao, B. Yang, and H. Cui, "Challenges and progresses of energy storage technology and its application in power systems," *Journal of Modern Power Systems and Clean Energy*, vol. 4, DOI 10.1007/s40565-016-0248-x, pp. 519–528, 2016.

[2] C. Blanc and A. Rufer, "Optimization of the operating point of a vanadium redox flow battery," in *2009 IEEE Energy Conversion Congress and Exposition*, DOI 10.1109/ECCE.2009.5316566, pp. 2600–2605, 2009.

[3] T. Takahashi and B. Sato, "Battery pack and charging method," U.S. Patent 12/725,109, 2010.

[4] Z. Wang, Y. Wang, Y. Rong, Z. Li, and L. Fantao, "Study on the optimal charging method for lithium-ion batteries used in electric vehicles," *Energy Procedia*, vol. 88, DOI 10.1016/j.egypro.2016.06.127, pp. 1013–1017, 2016.

[5] Y. Li, X. Zhang, J. Bao, and M. Skyllas-Kazacos, "Studies on optimal charging conditions for vanadium redox flow batteries," *Journal of Energy Storage*, vol. 11, DOI 10.1016/j.est.2017.02.008, pp. 191–199, 2017.

[6] H. Cai, "Power tracking and state-of-energy balancing of an energy storage system by distributed control," *IEEE Access*, vol. 8, DOI 10.1109/ACCESS.2020.3024714, pp. 170 261–170 270, 2020.

[7] B. Khaki and P. Das, "Multi-objective optimal charging current and flow management of vanadium redox flow batteries for fast charging and energy-efficient operation," *Journal of Power Sources*, vol. 506, DOI 10.1016/j.jpowsour.2021.230199, p. 230199, 2021.

[8] M. Guarnieri, P. Alotto, and F. Moro, "Distributed and lumped parameter models for fuel cells," *Thermodynamics and Energy Engineering*, vol. 1, DOI 10.1016/j.jpowsour.2021.230199, 2019.

[9] T. Puleston, A. Clemente, R. Costa-Castelló, and M. Serra, "Modelling and estimation of vanadium redox flow batteries: A review," *Batteries*, vol. 8, DOI 10.3390/batteries8090121, p. 121, 09 2022.

[10] S. S. Madani, E. Schaltz, and S. K. Kær, "A review of different electric equivalent circuit models and parameter identification methods of lithium-ion batteries," *ECS Transactions*, vol. 87, DOI 10.1149/08701.0023ecst, no. 1, pp. 23–37, Nov. 2018.

[11] H. He, R. Xiong, and J. Fan, "Evaluation of lithium-ion battery equivalent circuit models for state of charge estimation by an experimental approach," *Energies*, vol. 4, DOI 10.3390/en4040582, no. 4, pp. 582–598, 2011.

[12] D. Dvorak, T. Bäuml, A. Holzinger, and H. Popp, "A comprehensive algorithm for estimating lithium-ion battery parameters from measurements," *IEEE Transactions on Sustainable Energy*, vol. 9, DOI 10.1109/TSTE.2017.2761406, no. 2, pp. 771–779, 2018.

[13] A. Cunha, J. Martins, N. Rodrigues, and F. P. Brito, "Vanadium redox flow batteries: a technology review," *International Journal of Energy Research*, vol. 39, DOI 10.1002/er.3260, no. 7, pp. 889–918, 2015.

[14] A. Clemente and R. Costa-Castelló, "Redox flow batteries: A literature review oriented to automatic control," *Energies*, vol. 13, DOI 10.3390/en13174514, p. 4514, 09 2020.

[15] M. Skyllas-Kazacos, M. Rychcik, R. G. Robins, A. G. Fane, and M. A. Green, "New all-vanadium redox flow cell," in *Journal of The Electrochemical Society*, vol. 133, DOI 10.1109/ISGTEurope.2014.7028780, no. 5, p. 1057, 1986.

[16] M. Skyllas-Kazacos and M. Kazacos, "State of charge monitoring methods for vanadium redox flow battery control," *Journal of Power Sources*, vol. 196, DOI 10.1016/j.jpowsour.2011.06.080, no. 20, pp. 8822 – 8827, 2011.

[17] A. Clemente, G. A. Ramos, and R. Costa-Castelló, "Voltage H_∞ control of a vanadium redox flow battery," *Electronics*, vol. 9, DOI 10.3390/electronics9101567, no. 10, 2020.

[18] P. Zsuzsa, R.-E. Precup, J. Tar, and M. Takács, "Use of multi-parametric quadratic programming in fuzzy control systems," *Acta Polytechnica Hungarica*, vol. 3, 07 2006.

[19] G. Rigatos, P. Siano, D. Selisteanu, and R. E. Precup, "Nonlinear optimal control of oxygen and carbon dioxide levels in blood," *Intelligent Industrial Systems*, vol. 3, DOI 10.1007/s40903-016-0060-y, no. 2, pp. 61–75, 10 2017.

[20] H. S. Sánchez, A. Visioli, and R. Vilanova, "Optimal nash tuning rules for robust pid controllers," *Journal of the Franklin Institute*, vol. 354, DOI https://doi.org/10.1016/j.jfranklin.2017.03.012, no. 10, pp. 3945–3970, 2017. [Online]. Available: https://www.sciencedirect.com/science/article/pii/S0016003217301497

[21] V. Antonucci, G. Artale, G. Brunaccini, G. Caravello, A. Cataliotti, V. Cosentino, D. Di Cara, M. Ferraro, S. Guaiana, N. Panzavecchia, F. Sergi, and G. Tinè, "Li-ion battery modeling and state of charge estimation method including the hysteresis effect," *Electronics*, vol. 8, DOI 10.3390/electronics8111324, no. 11, 2019.

[22] B. Xiong, J. Zhao, Y. Su, Z. Wei, and M. Skyllas-Kazacos, "State of charge estimation of vanadium redox flow battery based on sliding mode observer and dynamic model including capacity fading factor," *IEEE Transactions on Sustainable Energy*, vol. 8, DOI 10.1109/TSTE.2017.2699288, no. 4, pp. 1658–1667, 2017.

[23] A. Clemente, M. Montiel, F. Barreras, A. Lozano, and R. Costa-Castelló, "Experimental validation of a vanadium redox flow battery model for state of charge and state of health estimation," *Electrochimica Acta*, vol. 449, DOI 10.1016/j.electacta.2023.142117, p. 142117, 03 2023.

[24] S. K. Murthy, A. K. Sharma, C. Choo, and E. Birgersson, "Analysis of concentration overpotential in an all-vanadium redox flow battery," *Journal of The Electrochemical Society*, vol. 165, DOI 10.1149/2.0681809jes, no. 9, pp. A1746–A1752, 2018.

[25] A. Clemente, M. Montiel, F. Barreras, A. Lozano, and R. Costa-Castellò, "Vanadium redox flow battery state of charge estimation using a concentration model and a sliding mode observer," *IEEE Access*, DOI 10.1149/2.0681809jes, 05 2021.

[26] A. T. Glazkov, A. E. Antipov, D. V. Konev, R. D. Pichugov, M. M. Petrov, N. V. Kartashova, P. A. Loktionov, J. M. Averina, and I. I. Plotko, "Dataset of a vanadium redox flow battery 10 membrane-electrode assembly stack," *Data in Brief*, vol. 31, DOI 10.1016/j.dib.2020.105840, p. 105840, 2020.

[27] A. Clemente and R. Costa, "Flow controlling tuning for the voltage of a redox flow battery considering the effect of overpotentials," *26th IEEE International Conference on Emerging Technologies and Factory Automation*, vol. 1, DOI 10.1109/ETFA45728.2021.9613582, 2021.